

PACS : 72.40, 73.20

# Electronic properties of silicon surface at different oxide film conditions

**S.I. Kirillova, V.E. Primachenko, E.F. Venger, V.A. Chernobai**

*Institute of Semiconductor Physics, NAS Ukraine, 45 Prospect Nauki, 03028 Kyiv, Ukraine  
Tel.: (380-44) 265-63-32; Fax: (380-44) 265-83-42; E-mail:*

**Abstract.** We used measurements of temperature and electric field dependencies of surface photovoltage to study electronic properties of (100) *n*-silicon surface after its thermal and chemical oxidation, as well as after oxide films removal in HF. Measurements of surface photovoltage vs temperature curves revealed two peaks of the fast surface electron states (SES) density. They lie in the gap in the region of  $P_{b0}$ - and  $P_{b1}$ -centers manifestation. The parameters of SES systems that were determined from the surface photovoltage vs electric field curves differ substantially from those determined from the temperature dependencies of surface photovoltage. They depend on the silicon surface condition, material resistivity and temperature at which the measurements were made. This is because the SES systems in oxide films (that exchange electrons with silicon via transport mechanisms) affect the measurements of electric field dependence of surface photovoltage.

**Keywords:** silicon-silicon oxide interface, surface electron states, surface photovoltage.

Paper received 21.03.00; revised manuscript received 22.01.01; accepted for publication 16.02.01.

## 1. Introduction

Thermally oxidized silicon surface is a basis for modern semiconductor electronics. That is why there exist a lot of works dealing with investigation of this surface, in particular, at different conditions of its oxide film (see, e.g., [1-4]).

To determine parameters of the surface electron states (SES), most of authors measure some quantity (that characterizes the near-surface region of semiconductor) – say, capacitance, conductivity and surface photovoltage – as a function of external electric field. It seems to us that in this case not only the fast SES (located at the silicon-oxide interface) are involved, but also (partially) the electronic states located in the oxide film. This occurs via electron transport between the latter states and silicon. Such situation hampers interpretation of experimental results, as well as determination of SES parameters from them.

The same flaw is inherent also to another technique that is used to study the silicon-oxide interface, namely, deep level transient spectroscopy (DLTS) [5-9]. Indeed, in DLTS an electric field is applied to the silicon surface to enrich the interfacial states with charge carriers. But this field might charge not only the interfacial states but also those located in the oxide film. Besides, if a low-

field version of DLTS is used, then one may obtain wrong results. The reason is that the interfacial states are filled only partially, because their trapping cross section depends on temperature [9].

The authors of [10] have proposed another method to determine SES spectra, namely, photoluminescence spectroscopy of SES (PLS<sup>3</sup>). In this method no external electric field is applied to the semiconductor surface. However, when fitting the experimental results concerning the photoluminescence intensity dependence on silicon illuminance from laser, a number of unknown parameters are used. Among them are cross sections of electron and hole trapping by SES, as well as their dependence on SES energy. Therefore the above PLS<sup>3</sup> method can be used for qualitative estimations only.

In this work we used two methods to obtain SES distribution in the gap of *n*-silicon after its thermal or chemical oxidation, as well as after oxide film removal in HF. These are: (i) measurements of temperature dependence of surface photovoltage (without external electric field applied to the semiconductor surface) and (ii) measurements of surface photovoltage as a function of the applied external electric field (at different fixed temperatures). The result is that SES spectra obtained by using the above two techniques are quite different. The first technique (measurements of temperature dependence of

surface photovoltage) gives two peaks of SES density for both thermally and chemically oxidized *n*-silicon surface. They lie in the 0.22–0.32 eV range over the midgap  $E_i$ . Another method (measurements of surface photovoltage as a function of the applied external electric field) gives continuous SES spectra whose concentration is more than an order of magnitude over that given by the first method. In this case the SES energy distribution essentially depends on condition of the silicon oxide film, as well as temperature at which the measurements are made. Such results evidence that the states in the oxide films play a prominent role during measurements of the electric field dependence of surface photovoltage.

## 2. Experimental techniques

We investigated the (100) surface of *n*-Si samples whose resistivity was 10 W·cm. Thermal oxide film (300 nm thick) was grown at a temperature of 1150 °C using combined three-step oxidation in dry (10 min.), moist (12 min.) and dry (10 min.) oxygen. After studying a sample with thermally oxidized surface, we investigated the same sample but with actual surface. To this end thermal oxide layer was removed by etching in HF (48%) followed by a short-term (10 s) washing in distilled water. The thickness of a native oxide film on such an actual surface did not exceed 0.45 nm [4].

After measurements the sample was chemically oxidized in concentrated HNO<sub>3</sub> for 20 s to obtain a chemical oxide film 1.5 nm thick [11], and the measurements were performed. After this the sample was again treated in HF and washed in distilled water for a short time. Then we studied it as a sample with actual surface obtained after removal of chemical oxide.

We measured both temperature and electric field dependencies of surface (capacitance) photovoltage at high concentration of photo-generated electron-hole pairs in silicon. In these conditions there was no band bending at silicon surface [12]. This enabled us to determine the surface potential  $\phi_s$  of the studied silicon surface in darkness (i.e., before illumination) at different temperatures and external electric fields ( $\phi_s$  corresponds to the band bending  $q\phi_s$  where  $q$  is the electron charge.) To obtain  $\phi_s$  we multiplied the measured photovoltage by a calibrating coefficient of the measuring circuit. This coefficient was determined using a test electric pulse. It should be noted that at high level of charge carrier generation the Dember photovoltage is not essential since the electron and hole diffusion coefficients become equal due to electron-hole scattering [13].

The surface potential  $\phi_s$  vs temperature curves were taken in a cryostat (pressure of 10<sup>-4</sup> Pa) at lowering temperature from 300 down to 100 K. At a definite temperature an effect of photo-induced memory of the surface potential appeared for all conditions of the silicon surface. Therefore we measured  $\phi_s$  with the first light pulse and provided that the surface traps be emptied from the trapped holes [14]. The surface potential  $\phi_s$  vs external electric field curves were taken at several fixed tempera-

tures lying between 300 and 100 K. The  $\phi_s$  values were measured after applying an external voltage  $V$  across the measuring capacitor. (This voltage changed within the +400 ÷ -400 V range.) In this case the measurements were performed using the second light pulse in their train. This enabled us to exclude effect of the photo-induced memory due to traps filling with holes during condenser illumination with the first light pulse. Besides, this served to exclude non-equilibrium at voltages that depleted silicon of electrons. This fact is of significance at reduced temperatures [15].

## 3. Experimental results and discussion

1. Shown in Fig. 1 are the surface potential  $\phi_s$  vs temperature curves taken for thermally (curve 1) and chemically (curve 2) oxidized silicon surfaces, as well as actual surfaces after removal of thermal (curve 3) and chemical (curve 4) oxide films with HF. One can see that the surface potential  $\phi_s$  is negative in all cases. As follows from our calculations, this means that in the near-surface regions of silicon there are layers depleted in electrons. For the thermally oxidized surface this fact means that there is no considerable built-in positive charge in the oxide film [1]. This conclusion is supported by the fact that  $\phi_s$  values for curves 1 and 3 (the latter taken after removal of the oxide film) are close.

For all curves the magnitude of  $\phi_s$  grows when temperature goes down. This is related to fast SES filling with electrons due to Fermi level shifting towards conduction band. It should be noted that when temperature decreases, then the electron equilibrium is established between the silicon bulk and fast SES only (the latter are located at the semiconductor-oxide interface). Contrary to this, the slow SES (that are located in the oxide film) do not manage to reach equilibrium with the semiconductor bulk at cooling. The reasons for this are long-term character of their charging (with spending of high

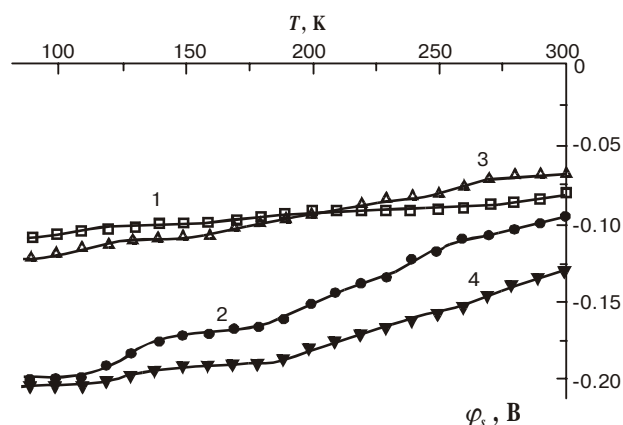


Fig. 1. Surface potential  $\phi_s$  vs temperature curves for thermally (1) and chemically (2) oxidized silicon surface; 3 and 4, respectively, the same after treatment of the above surfaces in HF.

activation energy [16]) and depletion of silicon surface. However, at room temperature the surface potential  $\varphi_s$  is determined by the total charge in both fast and slow SES. One can see from Fig. 1 that the biggest magnitude of this total charge (it should be noted that it is negative) is after treatment of the oxidized surface with HF.

A distinction between the slopes of  $\varphi_s(T)$  curves is due to different concentrations of fast SES at scanning by Fermi level of different portions of silicon gap at different oxide coatings of silicon surface. The minimal SES concentration (and, accordingly, the most gentle sloping of the  $\varphi_s(T)$  curve) is observed for thermally oxidized surface. And the most steeply sloping  $\varphi_s(T)$  curve is that for the chemically oxidized silicon surface.

2. A charge in the silicon near-surface region that corresponds to a definite value  $\varphi_s$  of surface potential is defined by the following expression [2]:

$$Q_{sv} = \sqrt{2}qn_iL \left\{ \lambda^{-1} \left[ \exp\left(\frac{q\varphi_s}{kT}\right) - 1 \right] + \lambda \left[ \exp\left(-\frac{q\varphi_s}{kT}\right) - 1 \right] + \frac{q\varphi_s}{kT} [\lambda - \lambda^{-1}] \right\}^{1/2} \quad (1)$$

Here  $L = (\varepsilon\varepsilon_0kT/q^2n_1)^{1/2}$ ;  $\lambda = n_1/n_0$ ;  $n_0$  ( $n_1$ ) is the electron concentration at a temperature  $T$  in the bulk of studied (intrinsic) material;  $k$  is the Boltzmann constant;  $\varepsilon$  is the silicon permittivity;  $\varepsilon_0 = 8.85 \cdot 10^{-12}$  F/m.

The total charge in SES,  $Q_s$ , is equal to the charge  $Q_{sv}$  with opposite sign. As was stated earlier,  $Q_s$  change with temperature is equal to change of charge in the fast SES only. One can pass from  $Q_s(T)$  dependencies to  $Q_s(\psi_s)$  curves where  $\psi_s = \varphi_b + \varphi_s$ .  $\varphi_s$  is measured, while  $\varphi_b$  can be determined for any temperature value  $T$  from the following expression:  $n_0 = n_1 \exp(q\varphi_b/kT)$ .  $q\varphi_b$  ( $q\psi_s$ ) is the energy differences between the midgap  $E_i$  and Fermi level in the silicon bulk (at the silicon surface). From  $Q_s(\psi_s)$  one can determine the fast SES density  $N_{sf}$  at various  $q\psi_s$  using the following expression:

$$N_{sf}(E) = |\Delta Q_s| / \Delta(q\psi_s) \quad (2)$$

Shown in Fig. 2 are the  $N_{sf}(E)$  curves for the surfaces studied in the 0.1 to 0.4 eV energy range over  $E_i$ . One can see that the SES density is minimal at the thermally oxidized surface (curve 1). There are two SES density peaks there, at energies  $E_i + 0.23$  eV and  $E_i + 0.32$  eV; the corresponding concentrations are  $6 \cdot 10^{10}$  and  $3.4 \cdot 10^{10}$   $\text{cm}^{-2} \cdot \text{eV}^{-1}$ . The SES density also increases at  $E > 0.36$  eV. For chemically oxidized surface (curve 2) the SES density is maximal. In this case there are also two peaks lying at the same (accuracy of 0.01 eV) energies as those for the thermally oxidized surface. The corresponding concentrations, however, are higher than in the previous case, namely,  $2.2 \cdot 10^{11}$  and  $1.8 \cdot 10^{11}$   $\text{cm}^{-2} \cdot \text{eV}^{-1}$ .

The fact that discrete SES lie at the same energies for both thermally and chemically oxidized silicon surfaces

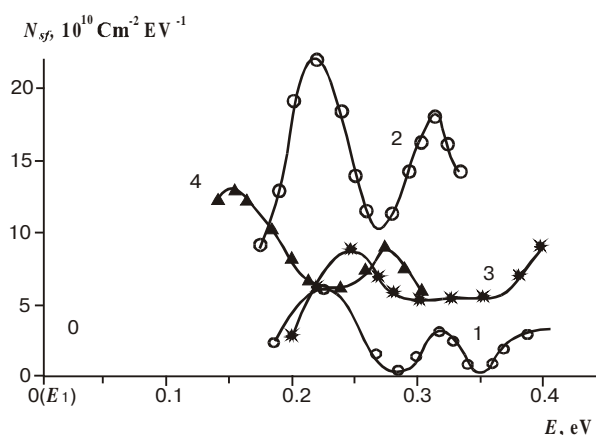


Fig. 2. Density of fast SES vs energy curves above the midgap  $E_i$  for thermally (1) and chemically (2) oxidized silicon surface; 3 and 4, respectively, the same after treatment of the above surfaces in HF.

serves as evidence that defects responsible for their appearance on these surfaces are of the same nature. We believe that these defects are  $P_{b0^-}$  and  $P_{b1^-}$ -centers that are registered on silicon (100) surface by electron paramagnetic resonance (EPR) [17, 18]. A  $P_{b0^-}$ -center is a trivalent silicon atom at the Si-SiO<sub>2</sub> interface. This atom is linked to three silicon atoms in the bulk. It has a free (dangling) orbital and is designated as Si<sub>3</sub>≡Si\*. Such a center is similar to  $P_b$ -center whose dangling orbital is normal to the silicon (111) surface [6, 18]. The nature of  $P_{b1^-}$ -center at the Si-SiO<sub>2</sub> interface has been discussed for a long time [4, 18-20]. The result was that it is a Si<sub>3</sub>≡Si\*-center too, but its dangling orbital is inclined by 20° to the (011) axis [21].

The investigations of the dependence of EPR signal at the silicon (100) surface on the external electric field (that charges  $P_{b0^-}$  and  $P_{b1^-}$ -centers with electrons) have shown that concentration peaks of these centers lie in the upper half of the gap, 0.28 and 0.23 eV over  $E_i$  [17, 18]. One should expect that at such energies the SES levels produced by  $P_{b0}$  and  $P_{b1}$  defects are to manifest themselves in electrical measurements. Instead of this, however, density of states has a broad peak in this portion of the gap. This result was obtained when studying the  $C-V$  curves. The corresponding concentration is about twice as large as the total concentration of the  $P_{b0^-}$  and  $P_{b1^-}$ -centers [17]. The explanation for this fact is as follows [18]. The investigation of the  $C-V$  curves detected not only the electronic states produced by the  $P_{b0^-}$  and  $P_{b1^-}$ -centers located at the Si-SiO<sub>2</sub> interface but also those in the oxide film. The latter states also exchange electrons with semiconductor at application of an external electric field. The states from the oxide film (that bear no relation to the  $P_{b0^-}$  and  $P_{b1^-}$ -centers) screen manifestation of the states produced by the above centers.

Later the electronic states (identified with the  $P_{b0^-}$  and  $P_{b1^-}$ -centers) in the Si-SiO<sub>2</sub> systems were studied using various electric methods. Among them were DLTS,

measurements of  $C$ - $V$  curves, measurements of MOS structures conductivity at alternating current –  $G$ - $V(\omega)$ . These methods were used immediately after MOS structure fabrication, as well as after the concentration of electronic states has been changed by radiation, strong electric fields, atomic hydrogen, annealing [7-9, 22-24]. For instance, in [24] a broad peak of the density of states was observed by measurements of  $C$ - $V$  curves for a MOS structure exposed to x-radiation. It lay in the region 0.2 to 0.3 eV over  $E_i$ . The method of  $G$ - $V(\omega)$  measurements revealed a peak lying at  $E_i + 0.32$  eV. In addition, a trend for peak appearance nearer to  $E_i$  was found. The authors of [8] applied to MOS structures high voltages resulting in appearance of SES. Using DLTS technique, they revealed a single peak of the SES density at  $E_i + 0.23$  eV. Nitration of oxide led to replacement of this single peak by another one lying at  $E_i + 0.35$  eV. In [23] it was stressed that whatever the method of defect production in MOS structures,  $P_b$ -centers are responsible for only a fraction of the density of states determined by electrical measurements. A considerable fraction of fast SES is located in the transition layer near the Si-SiO<sub>2</sub> interface.

The results obtained in [7] stand apart from the above. In this work the energy levels lying at  $E_i + 0.35$  and  $E_i + 0.15$  eV are ascribed to the  $P_{b0}$ - and  $P_{b1}$ -centers, respectively. The energy values were determined (immediately after MOS structure fabrication) with DLTS using small voltage pulses. These results do not agree with those obtained by all other authors. In particular, they predict no proximity (found in [17, 18]) in location of the  $P_{b0}$ - and  $P_{b1}$ -centers. It should be also noted that the energy position of the  $P_b$ -centers on the (111) surface obtained in [7] differs from that found in [6] (using the same DLTS technique). Such a feature of the results obtained in [7] might stem from not quite correct processing of the DLTS results. Indeed, it was shown in [9] where the energy spectrum of MOS structure on the (100) surface of  $p$ -Si was investigated with three methods ( $C$ - $V$  curves,  $G$ - $V(\omega)$  curves and DLTS using small voltage pulses) that the results obtained with DLTS have to be corrected due to both the temperature dependence of charge carrier trapping cross section and incomplete filling of the states during their charging.

Thus all the methods using external electric field could not separate two close electronic states in the energy range from 0.2 to 0.3 eV over  $E_i$ . In this range the  $P_{b0}$ - and  $P_{b1}$ -centers manifest themselves in EPR studies. We think that we could separate the above states in this work using a technique without electric field. Indeed, we revealed discrete levels lying 0.23 and 0.32 eV over  $E_i$ . They are related to the  $P_{b1}$ - and  $P_{b0}$ -centers, respectively.

One can see from Fig. 2 that after treatment in HF the SES density increases for the thermally oxidized surface (curve 3) and decreases for chemically oxidized surface (curve 4). The energy position of the SES density peaks also changes in this case. This seems to be due to the fact that after treatment in HF and short-term washing in water thin oxide films are formed. They have Si-H, Si-F and Si-OH bonds in large quantities [25, 26]. H and F atoms

and OH-groups located near trivalent silicon atoms may lead to change in energy levels produced by defects [27].

3. The above analysis has shown that when techniques using electric fields (even of low voltage) are applied, then charge carriers are partially trapped at the states in oxide films. This trapping becomes considerably more intense if one studies (at a definite temperature) dependence of the surface photovoltage on the voltage  $V$  applied across the measuring capacitor whose specific capacitance is  $C_d$ . To obtain SES density distribution, one should use the surface potential vs voltage curves,  $j_s(V)$ . From them the SES density was calculated at different  $j_s$  according to the following expression:

$$N_s(\varphi_s) = \left[ C_d \left( \frac{dV}{d\varphi_s} - 1 \right) - \frac{dQ_{sv}}{d\varphi_s} \right] / q. \quad (3)$$

One can pass from the  $N_s(\varphi_s)$  curves obtained at a definite temperature to the  $N_s(\psi_s)$  curves (or, what is the same, to the  $N_s(E)$  curves), just as it was made earlier.

Shown in Figs 3 and 4, 5 and 6 are the  $N_s(E)$  curves for the thermally oxidized and then treated in HF surfaces, as well as chemically oxidized and then treated in HF surfaces, respectively, at temperatures 290-130 K. One can see from Fig. 3 that for thermally oxidized surface the SES concentration in the energy range from -0.2 to +0.2 eV (relative to  $E_i$ ) does not depend on the temperature of measurement and lies within the  $(2-4) \cdot 10^{11} \text{ cm}^{-2} \cdot \text{eV}^{-1}$ . But in the region from 0.2 to 0.5 eV over  $E_i$  the SES concentration depends on the temperature of measurement. An abrupt rise in the SES concentration at higher temperatures begins at lower  $E$  (or  $\psi_s = \varphi_b + \varphi_s$ ). This increase of concentration  $N_s$  occurs when electric fields are applied to the silicon surface that enrich the near-surface region

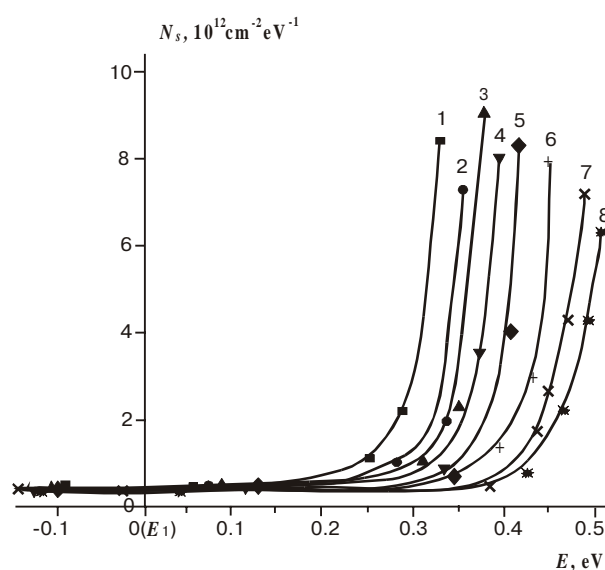
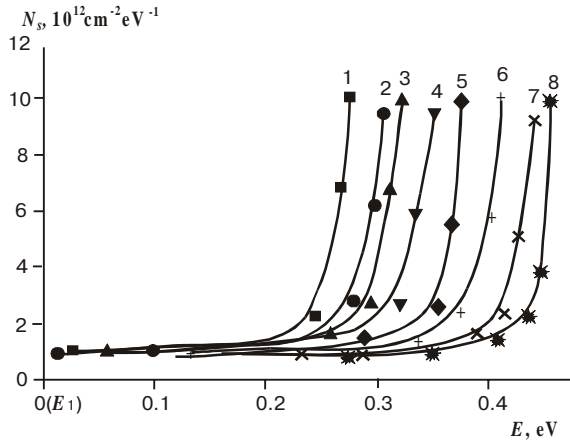
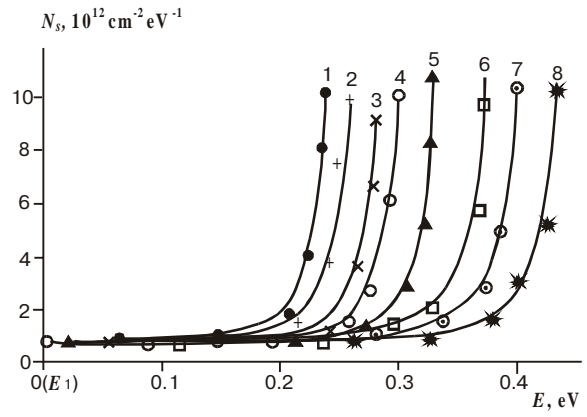


Fig. 3. Effective density of SES vs energy curves for thermally oxidized silicon surface at temperatures 290 (1), 270 (2), 255 (3), 230 (4), 205 (5), 185 (6), 150 (7) and 130 K (8).



**Fig. 4.** Effective density of SES vs energy curves for thermally oxidized and treated in HF silicon surface at temperatures 290 (1), 270 (2), 255 (3), 230 (4), 205 (5), 185 (6), 150 (7) and 130 K (8).



**Fig. 6.** The same as in Fig. 4 but for chemically oxidized and treated in HF silicon surface.

with electrons and increase  $\phi_s$ . The  $\phi_s$  values at which  $N_s$  abruptly increases are about the same at different temperatures. And shifting of the  $N_s$  growth beginning towards higher  $E$  when temperature goes down is due to  $\phi_b$  increase from 0.28 eV (at 290 K) to 0.47 eV (at 130 K).

From comparison between the  $N_{sf}(E)$  and  $N_s(E)$  dependencies (see Figs 2 and 3) obtained with two different methods for the thermally oxidized surface one can see the following. First, the above two curves have different SES distribution characters. The  $N_{sf}(E)$  dependence is discrete, while the  $N_s(E)$  one gives continuous SES distribution. Second, the SES concentration  $N_{sf}$  determined from the  $\phi_s(T)$  curves is by more than an order of magnitude below than the concentration  $N_s$  determined from the  $\phi_s(V)$  curves at different temperatures. The reason for

this is that  $N_{sf}$ , being determined in the absence of external electric fields, gives concentration of true fast SES only (they are at the Si-SiO<sub>2</sub> interface). But if one applies a technique that uses electric fields to determine  $N_s$ , then additional SES manifest themselves whose concentration is much over  $N_{sf}$ . They are located in the oxide film because there exist a considerably high electric field there that serves to transfer electrons between silicon and SES in oxide.

The electric field in the oxide film,  $\mathcal{E}_s$ , at inducing a charge  $Q_{ind}$  on silicon is given by the following expression (at the initial instant before a charge in SES begins to change):

$$\mathcal{E}_s = Q_{ind} / \epsilon_d \epsilon_0 = [Q_{sv}(\phi_{s0}) - Q_{sv}(\phi_s)] / \epsilon_d \epsilon_0. \quad (4)$$

Here  $\phi_{s0}$  ( $\phi_s$ ) is the silicon surface potential before (after) the external electric field is applied;  $\epsilon_d$  is the permittivity of silicon oxide. The charge  $Q_{sv}$  is negative (positive) when  $\phi_s > 0$  ( $\phi_s < 0$ ). According to expressions (1) and (4), if a voltage is applied to silicon that serves to deplete it of electrons, then the electric field  $\mathcal{E}_s$  in the oxide film is proportional to  $|q\phi_s/kT|^{1/2}$ . In our experiments  $\mathcal{E}_s$  was as high as  $3 \cdot 10^4$  V/cm. When the applied voltage serves to enrich silicon with electrons, then the electric field increases more abruptly:  $\mathcal{E}_s \propto \exp(q\phi_s/kT)$ . It follows from expressions (1) and (4) that an abrupt increase of  $\mathcal{E}_s$  occurs at lower temperatures and higher  $E = q\phi_s$  [29]. Thus a correlation exists between the curves  $\mathcal{E}_s(E)$  and  $N_s(E)$  in the enrichment region: at higher electric fields in the oxide film one obtains bigger determined effective SES density (that depends on the temperature of measurement).

There exist several different mechanisms for electron transfer between the semiconductor and SES in oxide [1, 2]. One of them is the tunnel mechanism for electron transfer from the silicon conduction band to the oxide electronic states at the Si-SiO<sub>2</sub> interface. Its role may be cru-

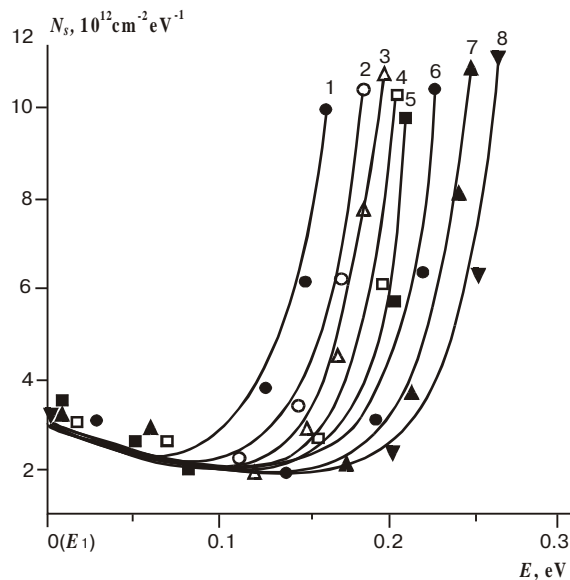


**Fig. 5.** The same as in Fig. 3 but for chemically oxidized silicon surface.

cial when one applies voltages serving to enrich silicon with electrons. Indeed, just after the electric field is applied, the rate of electrons trapping (via tunneling) at some oxide states whose concentration is  $N_{t0}$  is (ignoring backward tunneling from oxide to semiconductor)

$$\frac{dn_{t0}}{dt} \propto Dc_{n0}(N_{t0} - n_{t0})v_s n_s \quad (5)$$

Here  $c_{n0}$  is the effective cross section of electron trapping by oxide states;  $n_{t0}$  is the concentration of electrons in these states;  $n_s = n_0 \exp(q\phi_s/kT)$  is the concentration of electrons in conduction band near the semiconductor surface;  $v_s$  is the electron thermal velocity;  $D$  is the transparency coefficient for electrons tunneling from semiconductor to the oxide states. It is determined by the following expression:

$$D = D_0 \exp\left\{ -\frac{4\sqrt{2m}}{3\hbar} [(U - E_n)^{3/2} - (U - q\mathcal{E}_s d - E_n)^{3/2}] / q\mathcal{E}_s \right\} \quad (6)$$

Here  $D_0 = 1$ ;  $U$  is height of the potential barrier at the semiconductor-oxide interface;  $E_n$  is the tunneling electron energy;  $d$  is the spacing between the oxide states and semiconductor surface;  $m$  is the electron effective mass in oxide;  $\hbar$  is Planck's constant divided by  $2\pi$ .

According to expressions (5) and (6), application of voltages serving to silicon enrichment with electrons to the field electrode results in a considerable intensification of electron tunneling from the oxide SES. This is due to both growth of the transparency coefficient and increase of the electron concentration  $n_s$  near the silicon surface. The calculations show that the latter factor is of crucial importance since  $n_s$  grows exponentially with the surface potential  $\phi_s$ .

Electron tunneling to the oxide states results in a considerable growth of the SES effective density  $N_s$  (determined from the surface photovoltage measurements using electric fields) in the energy range from 0.2 to 0.5 eV over  $E_i$  (see Fig. 3). The true density  $N_{sf}$  of fast SES at the silicon-oxide interface (that is determined from the temperature dependencies of surface photovoltage in the energy range from 0.2 to 0.4 eV over  $E_i$ ) is less than  $N_s$  by more than an order of magnitude (see Fig. 2). It should be noted that during temperature measurements the silicon gap is studied in the mode of surface depletion of electrons. In this case electrons do not tunnel from silicon to the oxide SES, because there is no electric field in oxide (that could favor tunneling) and the  $n_s$  value is low.

After the thermal oxide film is etched away in HF, the character of  $N_s(E)$  curves remains principally the same (Fig. 4). In the region  $E < E_i + 0.2$  eV (that is studied at depleting voltages) the  $N_s$  value does not depend on the temperature of measurement. At  $E < E_i + 0.2$  eV (this energy region is studied at enriching voltages) the  $N_s$  value strongly depends on both  $E$  and the temperature of measurement. A thin actual oxide film, however, is structurally more imperfect than the thermal one. It has bigger number of electron states at a distance that electron can

overcome by tunneling. Therefore the effective SES density  $N_s$  on an actual surface (Fig. 4) is higher (at the same  $E$  and temperature) than that on chemically oxidized surface (Fig. 3).

After chemical oxidation of actual silicon surface the effective SES density considerably grows (Fig. 5). This is related to a thickness increase for the oxide film that contains a great number of defects. The latter trap charge from silicon when an external electric field is applied to it. One can see from Fig. 5 that the  $N_s$  value on chemically oxidized surface increases abruptly at enriching voltages due to electron tunneling from the conduction band to the oxide states. Besides, the  $N_s$  value considerably grows (as compared to the cases of thermally oxidized and actual surfaces) in the region of depleting voltages. This is evidence that electron transport between the oxide film and silicon occurs even at depleting electric fields due to various mechanisms [1, 2].

Subsequent treatment of chemically oxidized film in HF can serve to demonstrate a considerable contribution from defects in the oxide film to the determined  $N_s$  value. The  $N_s(E)$  curves obtained at different temperatures after treatment in HF (Fig. 6) are about the same as those obtained after thermal film removal with etching in HF. This means that removal of chemical oxide film considerably lowers the  $N_s$  values for definite  $E$  and  $T$  values.

## Conclusions

It follows from our work that SES parameters determined for the (100) surface of  $n$ -Si by two different methods of surface photovoltage measurements essentially depend on the character of its oxide coating.

The method of temperature dependence of photovoltage (when only fast SES at the silicon-oxide interface are studied) revealed two closely lying discrete SES levels. Their energy positions on thermally and chemically oxidized surfaces are the same, while concentrations differ (those on chemically oxidized surface are several times bigger). The origin of these states at the Si-SiO<sub>2</sub> interface seems to be related to the  $P_{b0}$ - and  $P_{b1}$ -centers. On actual silicon surfaces (obtained after removal of thermal and chemical oxide in HF) the SES concentration grows and drops, respectively, and the level energy positions shift.

The method of electric field dependence of photovoltage gave a continuous distribution of SES in the gap. Their effective concentration was an order of magnitude higher than that obtained by the first method. This is due to the fact that the second technique involves also the states of electrons in oxide films. A particularly abrupt increase of the SES effective concentration at enriching electric fields is related to realization of the tunneling mechanism for electron transport from the conduction band to silicon oxide states. The tunneling process depends on a number of parameters (in particular,  $\phi_s$  and  $\mathcal{E}_s$ ) of both semiconductor and oxide. Therefore the determined effective concentration of SES essentially depends on the semiconductor resistivity, temperature of measurements and oxide film condition. Of course, these

features of the determined effective parameters of SES exist not only at studies of the surface photovoltage dependence on electric field but also when studying other surface phenomena by the same method.

### Acknowledgements

The authors are grateful to V.Ya. Bratus and V.G. Litovchenko for valuable discussion of this work.

### References

1. V.G. Litovchenko, A.P. Gorban, *The Basics of Physics of the Microelectronic Metal-Insulator-Semiconductor Systems* (in Russian), Naukova Dumka, Kiev (1978).
2. *Properties of the Metal-Insulator-Semiconductor Structures* (in Russian), Ed. A.V. Rzhannov, Nauka, Moscow (1976).
3. V.F. Kiselev, *Surface Phenomena in Semiconductors and Insulators* (in Russian), Nauka, Moscow (1970).
4. *The Physics and Chemistry of SiO<sub>2</sub> and the Si-SiO<sub>2</sub> interface*. Proc. 3<sup>rd</sup> Intern. Symposium, Pennington, NJ (1996).
5. N.M. Johnson // *Appl. Phys. Lett.* **34**(11), p. 803 (1979).
6. N.M. Johnson, D.K. Biegelsen, M.D. Mayer et al. // *Appl. Phys. Lett.* **43**(6), p. 563 (1983).
7. D. Vuillaume, D. Goguenheim, G. Vincent // *Appl. Phys. Lett.* **57**(12), p. 1206 (1990).
8. S. Belkouch, C. Jean, C. Aktik // *Appl. Phys. Lett.* **67**(4), p. 530 (1995).
9. S. Ozder, I. Atilgan, B. Katircioglu // *Semicond. Sci. Technol.* **10**(11), p. 1510 (1995).
10. S. Koyanagi, T. Hashizme, H. Hasegawa // *Jpn. J. Appl. Phys.* **35**(2B), p. 946 (1996).
11. K. Prabharan, Y. Kobayashi, T. Ogino // *Surf. Sci.* **290**(3), p. 239 (1993).
12. A.V. Sachenko, O.V. Snitko, *Photoeffects in Semiconductor Near-surface Layers* (in Russian), Naukova Dumka, Kiev (1984).
13. Z.S. Gribnikov, V.I. Melnikov // *Fiz. Tekhn. Poluprov.* **2**(6), p. 1352 (1968).
14. S.I. Kirillova, V.E. Primachenko, V.A. Chernobai // *Optoelektronika i Poluprovodnikovaya Tekhnika* No 21, p. 60 (1991).
15. V.E. Primachenko, O.V. Snitko, V.V. Milenin // *phys. stat. sol.* **11**(3), p. 711 (1965).
16. V.F. Kiselev, S.N. Kozlov // *Poverknost* No 2, p. 13 (1982).
17. G.J. Gerardi, E.H. Poindexter, P.J. Caplan, N.M. Johnson // *Appl. Phys. Lett.* **49**(6), p. 348 (1986).
18. E.H. Poindexter // *Semicond. Sci. Technol.* **4**(5), p. 961 (1989).
19. J.H. Stathis, L. Dorl // *Appl. Phys. Lett.* **58**(15), p. 1641 (1991).
20. A. Stesmans // *Solid State Commun.* **97**(4), p. 255 (1996).
21. A. Stesmans, B. Nouwen, V.V. Afanas'ev // *J. Phys.: Condens. Matter* **10**(27), p. L495 (1998).
22. L.-A. Ragnarsson, P. Lundgren, Z. Ovuka, M.O. Andersson, in *The Physics and Chemistry of SiO<sub>2</sub> and the Si-SiO<sub>2</sub> interface*. Proc. 3<sup>rd</sup> Intern. Symposium, Pennington, NJ, p. 667 (1996).
23. R.E. Stahlbush, in *The Physics and Chemistry of SiO<sub>2</sub> and the Si-SiO<sub>2</sub> interface*. Proc. 3<sup>rd</sup> Intern. Symposium, Pennington, NJ, p. 525 (1996).
24. N. Haneji, L. Vishnubhota, T. Ma // *Appl. Phys. Lett.* **59**(26), p. 3416 (1991).
25. G.J. Pietsch // *Appl. Phys.* **A60**(4), p. 347 (1995).
26. K. Ljungberg, A. Soderbarg, U. Jansson // *Appl. Phys. Lett.* **67**(5), p. 65 (1995).
27. T. Sakurai, T. Sugano // *J. Appl. Phys.* **52**(11), p. 2889 (1981).
28. Y.W. Lam // *J. Phys. D: Appl. Phys.* **42**(4), p. 1370 (1971).
29. S.I. Kirillova, V.E. Primachenko, V.A. Chernobai // *Fiz. Tekhn. Poluprov.* **30**(1), p. 118 (1996).